

AFWL-TR-76-333

AFWL-TR-
76-333

AD A040267

**ELECTROMAGNETIC COUPLING BETWEEN
MULTICONDUCTOR TRANSMISSION LINES
IN A HOMOGENEOUS MEDIUM**

Science Applications, Inc.
Berkeley, CA 94701

May 1977

Final Report

Approved for public release; distribution unlimited.

AD No. _____
DDC FILE COPY



AIR FORCE WEAPONS LABORATORY
Air Force Systems Command
Kirtland Air Force Base, NM 87117



This final report was prepared by Science Applications, Inc., Berkeley, California, under Contract F29601-76-C-0125, Job Order 12090513 with the Air Force Weapons Laboratory, Kirtland Air Force Base, New Mexico. Capt M. G. Harrison was the Laboratory Project Officer-in-Charge.

When US Government drawings, specifications, or other data are used for any purpose other than a definitely related Government procurement operation, the Government thereby incurs no responsibility nor any obligation whatsoever, and the fact that the Government may have formulated, furnished or in any way supplied the said drawings, specifications, or other data is not to be regarded by implication or otherwise as in any manner licensing the holder or any other person or corporation or conveying any rights or permission to manufacture, use, or sell any patented invention that may in any way be related thereto.

This report has been reviewed by the Office of Information (OI) and is releasable to the National Technical Information Service (NTIS). At NTIS, it will be available to the general public, including foreign nations.

This technical report has been reviewed and is approved for publication.

Michael G. Harrison

MICHAEL G. HARRISON
Captain, USAF
Project Officer

FOR THE COMMANDER

Aaron B. Loggins

AARON B. LOGGINS
Lt Colonel, USAF
Ch, Phenomenology & Technology Branch

James L. Griggs, Jr.

JAMES L. GRIGGS, JR.
Colonel, USAF
Ch, Electronics Division

Form with distribution and availability codes, including fields for NTIS, DTIC, and other agencies. A large 'A' is handwritten in the bottom right corner.

DO NOT RETURN THIS COPY. RETAIN OR DESTROY.

UNCLASSIFIED

SECURITY CLASSIFICATION OF THIS PAGE (When Data Entered)

REPORT DOCUMENTATION PAGE		READ INSTRUCTIONS BEFORE COMPLETING FORM
1. REPORT NUMBER AFWL-TR-76-333	2. GOVT ACCESSION NO.	3. RECIPIENT'S CATALOG NUMBER
4. TITLE (and Subtitle) ELECTROMAGNETIC COUPLING BETWEEN MULTICONDUCTOR TRANSMISSION LINES IN A HOMOGENEOUS MEDIUM.		5. TYPE OF REPORT & PERIOD COVERED Final Report
7. AUTHOR(s) Tom K./Liu		6. PERFORMING ORG. REPORT NUMBER
9. PERFORMING ORGANIZATION NAME AND ADDRESS Science Applications, Inc. Berkeley, CA 94701		8. CONTRACT OR GRANT NUMBER(s) F29601-76-C-0125 new
11. CONTROLLING OFFICE NAME AND ADDRESS Air Force Weapons Laboratory (ELPE) Kirtland Air Force Base, NM 87117		10. PROGRAM ELEMENT, PROJECT, TASK AREA & WORK UNIT NUMBERS 64747F 12090513
14. MONITORING AGENCY NAME & ADDRESS (if different from Controlling Office)		12. REPORT DATE May 1977
		13. NUMBER OF PAGES 49 p.
		15. SECURITY CLASS. (of this report) UNCLASSIFIED
16. DISTRIBUTION STATEMENT (of this Report) Approved for public release; distribution unlimited.		
17. DISTRIBUTION STATEMENT (of the abstract entered in Block 20, if different from Report)		
18. SUPPLEMENTARY NOTES		
19. KEY WORDS (Continue on reverse side if necessary and identify by block number) Transmission Lines; Multiconductor Transmission Lines; Transmission Line Coupling; Electromagnetic Pulse (EMP) Coupling to Transmission Lines		
20. ABSTRACT (Continue on reverse side if necessary and identify by block number) (UNCLASSIFIED ABSTRACT) The electromagnetic coupling between multiconductor transmission lines which are immersed in a homogeneous medium are investigated in this report. The method of reflection matrices is used to show how the line voltages and currents are related to the driving source voltages or currents. It is also shown that for weak coupling, the expressions for the induced voltages and currents on a conductor due to energy on another conductor may be greatly simplified. In fact, the effect of the crosscoupling can be represented by lumped voltage and/or current generators on the induced conductor.		

CONTENTS

<u>Section</u>	<u>Page</u>
I. INTRODUCTION	5
II. GENERAL FORMULATION	6
1. Voltage-Driven Lines	8
2. Current-Driven Lines	12
III. THREE-CONDUCTOR TRANSMISSION LINES-- SPECIAL CASES	15
1. Analytical Results	18
(a) Matched Lines	18
(b) Short-Circuit Loads	21
2. Numerical Results	22
IV. EQUIVALENT GENERATORS REPRESENTATION OF CROSS-COUPLING	29
1. Formulation	30
2. Comparison with Exact Theory	42
V. CONCLUSIONS	45
REFERENCES	47

ILLUSTRATIONS

<u>Figure</u>		<u>Page</u>
1	Voltage-driven (n+1)-conductor transmission lines	9
2	Current-driven (n+1)-conductor transmission lines	13
3	Coupling coefficient of two identical circular cylinders above a ground plane	17
4	(a) Voltage-driven matched three-conductor transmission lines, (b) Circuit representation of characteristic impedance matrix \bar{Z}_0 , (c) Circuit representation of matched three-conductor transmission line	20
5	Three-conductor transmission line configurations for numerical studies	24
6	The case $R_S = R_L = 50\Omega$ at 100MHz. (a) Voltages and currents at $z = 0$, and (b) Voltages at $z = l$.	25
7	The case $R_S = 50\Omega$, $R_L = 100\Omega$ at 100 MHz. (a) Voltages at $z = 0$, and (b) Voltages at $z = l$.	26
8	The case $R_S = 50\Omega$, $R_L = 100\Omega$ for $k = 0.1$. (a) Voltages and Currents at $z = 0$, and (b) Voltages at $z = l$.	28
9	Three-conductor transmission line terminated in simple impedances	31
10	A pair of voltage generators $V_\xi/2$ and a current generator I_ξ at $z = \xi$.	33
11	Three possible equivalent generator representations of cross-coupling: (a) three voltage generators, (b) one voltage and one current generator, and (c) two voltage and two current generators	37
12	Two-voltage generator representation of effect of voltage and current of line 1 on line 2	40

ILLUSTRATIONS (cont'd.)

Figure

Page

- 13 Comparisons of exact and approximate results. (a) $R_s = R_\ell = 50\Omega$, and
(b) $R_s = 50\Omega$ and $R_\ell = 100\Omega$.

44

SECTION I

INTRODUCTION

In many practical configurations of multiconductor transmission lines, as encountered in the study of electromagnetic pulse (EMP) internal interaction problems, the conductors are covered by thin dielectric jackets. The associated propagation modes (ref. 1) are thus approximately degenerate and can be understood by studying the propagation problems of multiconductor transmission lines in homogeneous media.

Of particular interest are the studies of electromagnetic coupling among the conductors (or lines), which would reveal how the energy on one line affects another. In this report, we study the coupling problem of an $(n+1)$ -conductor uniform transmission line imbedded in a homogeneous medium. The $(n+1)^{\text{st}}$ conductor is referred to as the reference conductor (usually a ground plane or the overall shield). The special case $n = 2$ will be studied in detail.

The voltages and currents along the lines for a given set of termination conditions are expressed in terms of reflection matrices. This formulation, as reported in Section II, enables one to observe the effects of terminations on the coupling among the lines. The special cases of three conductor lines are presented in Section III. Finally, we show that in the case of weak coupling among two parallel lines, the effect of one line can be represented by equivalent generators on the other line.

SECTION II

GENERAL FORMULATION

In this section, expressions for line voltages and currents on an $(n+1)$ -conductor transmission line immersed in a homogeneous medium are derived. Two specific sets of termination conditions are used; one involves driving the conductors at one end by voltage sources through an impedance network, whereas the other involves driving by current sources through an admittance network. Specialization of the results to the three-conductor transmission line case is presented in Section III.

The starting point of the derivation is the familiar set of $2n$ transmission line equations in matrix form for the voltage vector $\bar{V}(z)$ and current vector $\bar{I}(z)$ at a position z , viz.:

$$\frac{d}{dz} \begin{bmatrix} \bar{V}(z) \\ \bar{I}(z) \end{bmatrix} = -s \begin{bmatrix} \bar{0} & \bar{L} \\ \bar{C} & \bar{0} \end{bmatrix} \begin{bmatrix} \bar{V}(z) \\ \bar{I}(z) \end{bmatrix} \quad (1)$$

where s is the complex frequency, $\bar{0}$ is the $n \times n$ zero matrix, \bar{L} and \bar{C} are respectively the per-unit-length

inductance matrix and the per-unit-length capacitance matrix. Both \bar{L} and \bar{C} are $n \times n$ square matrices.

It is to be noted that the matrix $\bar{C} = [C_{ij}]$ is defined so that

$$Q_i = \sum_{j=1}^n C_{ij} V_j \quad i=1,2,\dots,n$$

where Q_i is the charge on line i and V_j is the potential of line j with respect to the reference conductor. Often (ref. 2) C_{ii} is called the coefficient of self-capacitance and C_{ij} , $i \neq j$, is called the coefficient of inductance.

For a homogeneous medium, it can be shown (refs. 3, 4) that

$$\bar{L} \bar{C} = \bar{C} \bar{L} = \frac{1}{v^2} \bar{U}_n \quad (2)$$

where v is the speed of light in the medium and \bar{U}_n is the $n \times n$ unity matrix, i.e., a diagonal matrix with all diagonal elements being 1. Equation (2) indicates that the eigenvalues of the square matrix in (1) are degenerate.

Differentiating (1) with respect to z yields

$$\frac{d^2}{dz^2} \begin{bmatrix} \bar{V}(z) \\ \bar{I}(z) \end{bmatrix} = \gamma^2 \begin{bmatrix} \bar{V}(z) \\ \bar{I}(z) \end{bmatrix} \quad (3)$$

where the propagation constant is given by

$$\gamma = s/v$$

The solution of the second equation in (3) can be expressed in terms of two travelling waves, viz.,

$$\bar{I}(z) = e^{-\gamma z} \bar{I}^+ + e^{\gamma z} \bar{I}^- \quad (4)$$

where the amplitude vectors \bar{I}^+ and \bar{I}^- are determined from termination conditions. Substituting (4) in (1), we obtain

$$\bar{V}(z) = \bar{Z}_0 \left(e^{-\gamma z} \bar{I}^+ - e^{\gamma z} \bar{I}^- \right) \quad (5)$$

where \bar{Z}_0 is the characteristic impedance matrix (ref. 1) and is given by

$$\bar{Z}_0 = \frac{1}{v} \bar{C}^{-1} = v \bar{L} \quad (6)$$

1. Voltage-Driven Lines

Let us assume that the lines are driven by a voltage source array \bar{V}_s at $z = 0$ through an impedance network \bar{Z}_s , and are terminated at $z = \ell$ by another impedance network \bar{Z}_ℓ . These termination conditions are depicted in Figure 1 and are described by

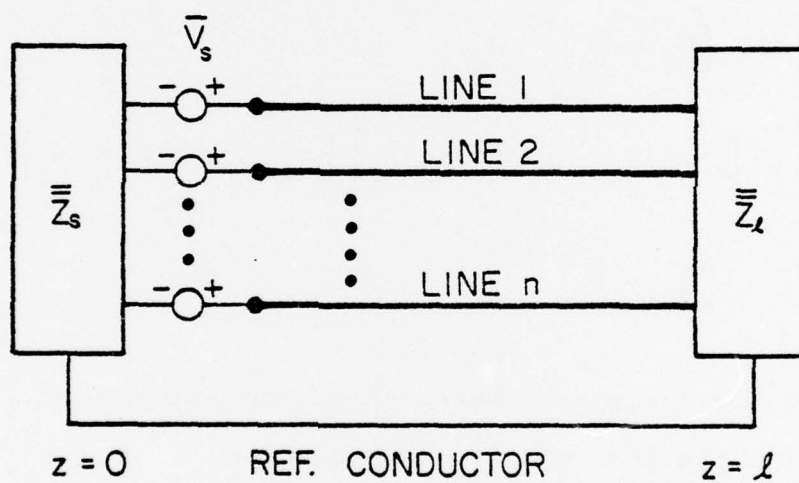


Figure 1. Voltage-driven (n+1)-conductor transmission lines.

$$\begin{aligned}\bar{V}(0) &= \bar{V}_s - \bar{Z}_s \bar{I}(0) \\ \bar{V}(\ell) &= \bar{Z}_\ell \bar{I}(\ell)\end{aligned}\tag{7}$$

Solution of (4) and (5) together with (7) yields

$$\begin{aligned}\bar{V}(z) &= \bar{Z}_0 \left[e^{-\gamma z} \bar{U}_n + e^{\gamma(z-2\ell)} \bar{\Gamma}_\ell \right] \left[\bar{U}_n - e^{-2\gamma\ell} \bar{\Gamma}_s \bar{\Gamma}_\ell \right]^{-1} \\ &\quad \left[\bar{Z}_s + \bar{Z}_0 \right]^{-1} \bar{V}_s \\ \bar{I}(z) &= \left[e^{-\gamma z} \bar{U}_n - e^{\gamma(z-2\ell)} \bar{\Gamma}_\ell \right] \left[\bar{U}_n - e^{-2\gamma\ell} \bar{\Gamma}_s \bar{\Gamma}_\ell \right]^{-1} \\ &\quad \left[\bar{Z}_s + \bar{Z}_0 \right]^{-1} \bar{V}_s\end{aligned}\tag{8}$$

where the reflection matrices at the source end $\bar{\Gamma}_s$ and at the load end $\bar{\Gamma}_\ell$ are given by

$$\begin{aligned}\bar{\Gamma}_s &= [\bar{Z}_s + \bar{Z}_0]^{-1} [\bar{Z}_s - \bar{Z}_0] \\ \bar{\Gamma}_\ell &= [\bar{Z}_\ell + \bar{Z}_0]^{-1} [\bar{Z}_\ell - \bar{Z}_0]\end{aligned}\tag{9}$$

For multiconductor transmission lines, \bar{Z}_0 is usually a full, asymmetric matrix. Hence, in general, $[\bar{Z}_s + \bar{Z}_0]$, $\bar{\Gamma}_s$ and $\bar{\Gamma}_\ell$ are not diagonal matrices. This

fact implies that $\bar{V}(z)$ is related to \bar{V}_s by a full matrix and hence cross-coupling occurs, i.e., the voltage source on one line causes induction of voltages on all other lines. Similarly, the current $\bar{I}(z)$ is also coupled to \bar{V}_s . One exception is the condition that the lines are perfectly terminated, i.e., $\bar{\Gamma}_s = \bar{\Gamma}_\ell = \bar{0}$, or $\bar{Z}_s = \bar{Z}_\ell = \bar{Z}_0$ (this demands all interconductor elements of the source and load impedance networks match the corresponding ones of the characteristic impedance), then

$$\begin{aligned}\bar{V}(z) &= \frac{1}{2} e^{-\gamma z} \bar{V}_s \\ \bar{I}(z) &= \frac{1}{2} e^{-\gamma z} \bar{Z}_0^{-1} \bar{V}_s\end{aligned}\tag{10}$$

Equation (10) states that under the matched condition, the line voltages are not cross-coupled to the driving voltage sources, whereas the currents are. This situation can be explained from a circuit-theory point-of-view. Such an explanation for a three-wire line is presented in Section III.

Equation (10) points to the conditions of producing pure voltage modes when each conductor is excited by a voltage source connecting the conductor to the reference conductor. When the lines are perfectly matched at both

ends, no cross-coupling of voltages occur. However, cross-coupling occurs if discontinuities exist along the line or at the two terminating ends. We observe also that pure current modes are not excited by this type of source arrangements.

2. Current-Driven Lines

Here we assume that the lines are driven by a current source array \bar{I}_s through an admittance network \bar{Y}_s at $z = 0$ and are terminated by an admittance \bar{Z}_ℓ at $z = \ell$. This arrangement is depicted in Figure 2. In this case, we have

$$\begin{aligned}\bar{V}(0) &= \bar{Y}_s^{-1} [\bar{I}_s - \bar{I}(0)] \\ \bar{V}(\ell) &= \bar{Z}_\ell \bar{I}(\ell)\end{aligned}\tag{11}$$

Solution of (4) and (5) together with termination conditions of equation (11) yields

$$\begin{aligned}\bar{V}(z) &= \bar{Z}_0 \left[e^{-\gamma z} \bar{U}_n + e^{\gamma(z-2\ell)} \bar{I}_\ell \right] \left[\bar{U}_n - e^{-2\gamma\ell} \bar{I}_s \bar{I}_\ell \right]^{-1} \\ &\quad \left[\bar{Y}_s^{-1} + \bar{Z}_0 \right]^{-1} \bar{Y}_s^{-1} \bar{I}_s\end{aligned}$$

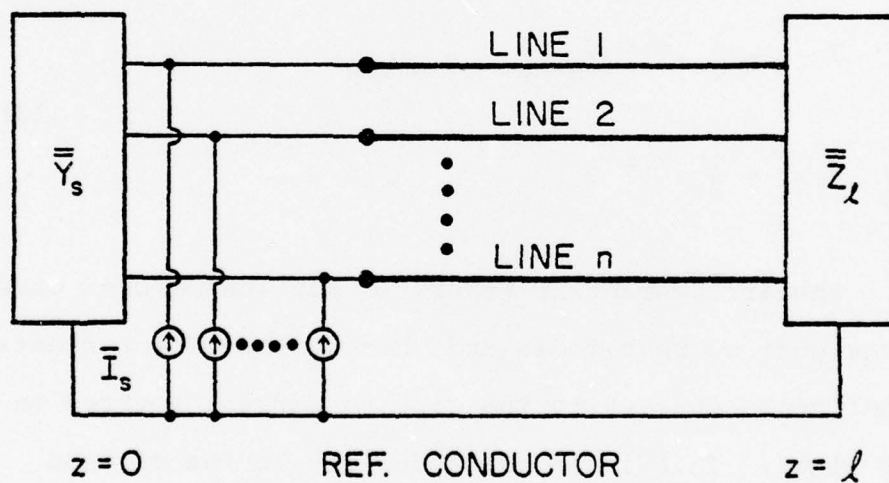


Figure 2. Current-driven (n+1)-conductor transmission lines.

$$\bar{I}(z) = \left[e^{-\gamma z} \bar{U}_n - e^{\gamma(z-2\ell)} \bar{I}_\ell \right] \left[\bar{U}_n - e^{-2\gamma\ell} \bar{I}_s \bar{I}_\ell \right]^{-1} \\ \left[\bar{Y}_s^{-1} + \bar{Z}_o \right]^{-1} \bar{Y}_s^{-1} \bar{I}_s \quad (12)$$

Here \bar{I}_s is the same as in (9) should one take $\bar{Z}_s = \bar{Y}_s^{-1}$. We observe again that both the line voltages and currents are cross-coupled to the source \bar{I}_s .

Again, for the matched case, i.e., $\bar{I}_s = \bar{I}_\ell = \bar{0}$, we have

$$\bar{V}(z) = \frac{1}{2} e^{-\gamma z} \bar{Z}_o \bar{I}_s \\ \bar{I}(z) = \frac{1}{2} e^{-\gamma z} \bar{I}_s \quad (13)$$

The arrangement in Figure 2, for the matched case, excites pure current modes and, hence, the line currents are not cross-coupled to the driving current sources on other lines. This is in exact duality to the matched case discussed for the voltage-driven lines.

SECTION III

THREE-CONDUCTOR TRANSMISSION LINES--SPECIAL CASES

The study of a three-conductor transmission line (including the reference conductor) is very important in understanding the coupling mechanisms of multiconductor transmission lines, particularly if the coupling between conductors is weak. For weak coupling, the effect of coupling from other lines can be obtained by using superpositions of coupling from individual lines--i.e., superimposing the results of three-conductor transmission lines.

For a three-conductor transmission line, the per-unit-length inductance matrix $\bar{\bar{L}}$ and per-unit-length capacitance matrix $\bar{\bar{C}}$ can be written as

$$\bar{\bar{L}} = \begin{bmatrix} L_{11} & L_m \\ L_m & L_{22} \end{bmatrix} \quad (14)$$

and

$$\bar{\bar{C}} = \begin{bmatrix} C_{11} & -C_m \\ -C_m & C_{22} \end{bmatrix} \quad (15)$$

where the subscripts 11, 22 and m denote self-quantities for lines 1 and 2, and the mutual quantities between lines 1 and 2, respectively. Condition (2) for homogeneous media results in the following relations:

$$\frac{L_m}{C_m} = \frac{L_{11}}{C_{22}} = \frac{L_{22}}{C_{11}} = v^2 (L_{11} L_{22} - L_m^2) = \frac{1}{v^2 (C_{11} C_{22} - C_m^2)} \quad (16)$$

To get an idea of the relative magnitudes of the mutual and self-quantities, the coupling coefficient k of two identical circular cylinders of radius r , center-to-center separation $2a$, and parallel to a ground plane (which serves as the reference conductor) at a height b (center-to-ground plane) is evaluated. The coupling coefficient is defined to be

$$k = \frac{C_m}{\sqrt{C_{11} C_{22}}} \quad (17)$$

and is given by (ref. 5)

$$k = \frac{\ln [1 + (b/a)^2]}{2 \ln (2b/r)}$$

In Figure 3, the coupling coefficient is plotted versus a/b for various b/r . For this configuration, it is observed that the maximum value of k is 0.5 and occurs when the two conductors are about touching each other and also about touching the ground plane. When the conductors are of different sizes, higher values of k are possible.

From (6), the elements of the characteristic impedance matrix are readily expressible in terms of the \bar{C} and \bar{L} elements. For

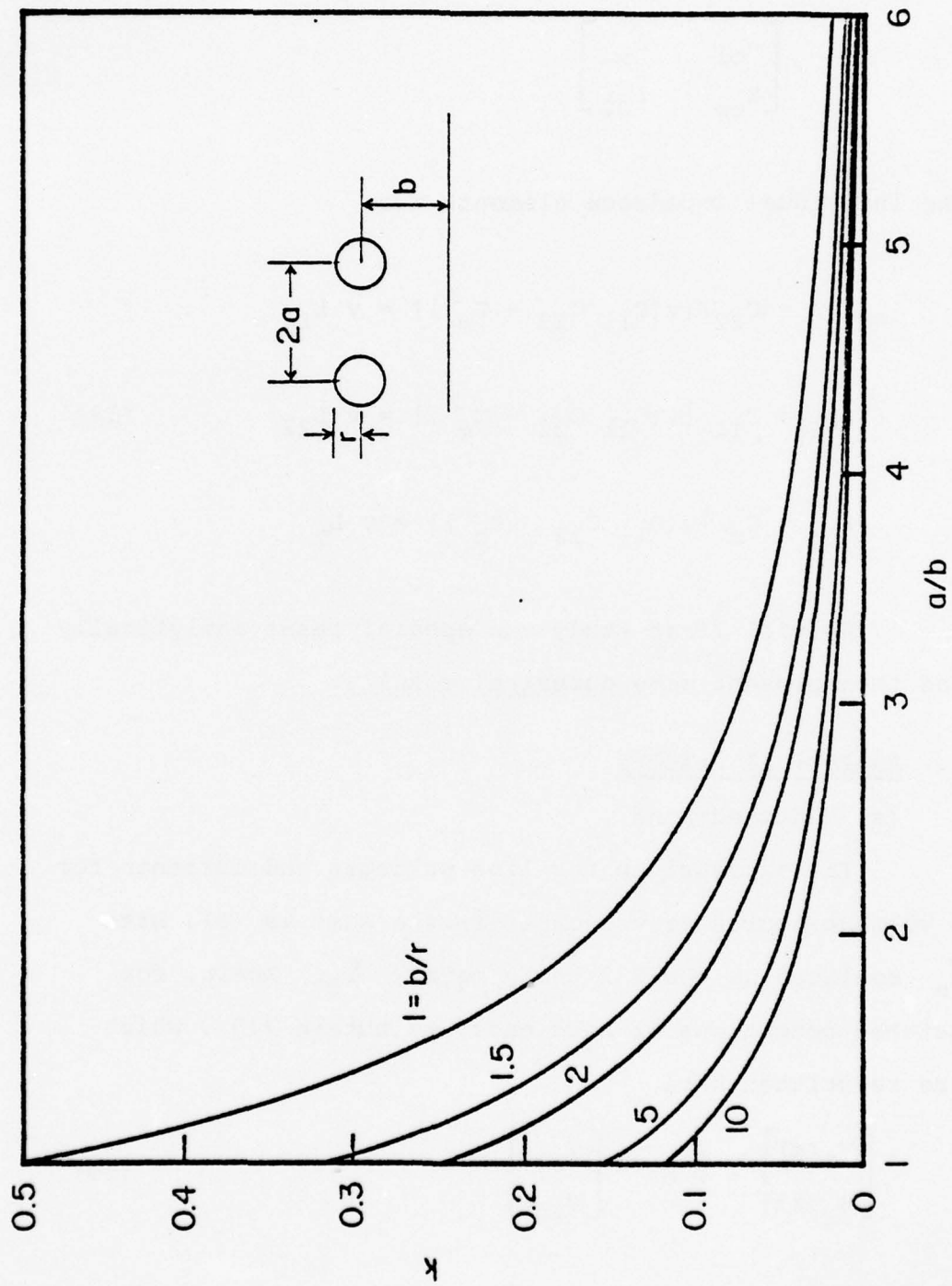


Figure 3. Coupling coefficient of two identical circular cylinders above a ground plane.

$$\bar{\bar{Z}}_0 = \begin{bmatrix} Z_{01} & Z_{0m} \\ Z_{om} & Z_{02} \end{bmatrix}$$

the individual impedance elements are

$$\begin{aligned} Z_{01} &= C_{22} / [v(C_{11} C_{22} - C_m^2)] = v L_{11} \\ Z_{02} &= C_{11} / [v(C_{11} C_{22} - C_m^2)] = v L_{22} \\ Z_{om} &= C_m / [v(C_{11} C_{22} - C_m^2)] = v L_m \end{aligned} \quad (18)$$

We will first study two special cases analytically and then present some numerical results.

1. Analytical Results

(a) Matched Line

The expressions for line voltages and currents for a voltage-source driven case are the same as (8), with $\bar{\bar{U}}_n$ replaced by the 2×2 unity matrix $\bar{\bar{U}}_2$. Again, for matched conditions at both ends, we obtain (10), which are re-written here

$$\begin{bmatrix} V_1(z) \\ V_2(z) \end{bmatrix} = \frac{1}{2} e^{-\gamma z} \begin{bmatrix} V_{s1} \\ V_{s2} \end{bmatrix} \quad (19)$$

and

$$\begin{bmatrix} I_1(z) \\ I_2(z) \end{bmatrix} = \frac{1}{2} e^{-\gamma z} \begin{bmatrix} z_{01} & z_{om} \\ z_{om} & z_{o2} \end{bmatrix}^{-1} \begin{bmatrix} v_{s1} \\ v_{s2} \end{bmatrix}$$

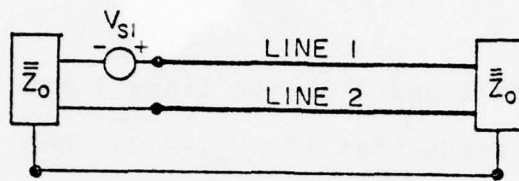
where subscripts 1 and 2 denote lines 1 and 2, respectively. Equations (19) state that if $v_{s2} = 0$, then

$$\begin{aligned} v_1(z) &= \frac{1}{2} e^{-\gamma z} v_{s1} \\ v_2(z) &= 0 \\ I_1(z) &= \frac{1}{2} e^{-\gamma z} v_{s1} z_{o2} / (z_{o1} z_{o2} - z_{om}^2) \\ I_2(z) &= -\frac{1}{2} e^{-\gamma z} v_{s1} z_{om} / (z_{o1} z_{o2} - z_{om}^2) \end{aligned} \tag{20}$$

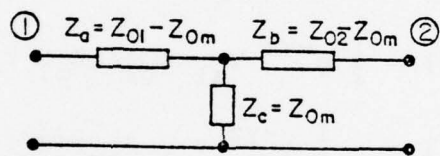
It is also possible to obtain (20) using circuit-analysis techniques.

The voltage-driven matched three-conductor transmission line is shown in Figure 4a, and the circuit representation (ref. 6) of the characteristic impedance matrix $\bar{\bar{z}}_o$ is shown in Figure 4b. The complete representation in circuit form of the matched transmission line at $z = 0$ is shown in Figure 4c.

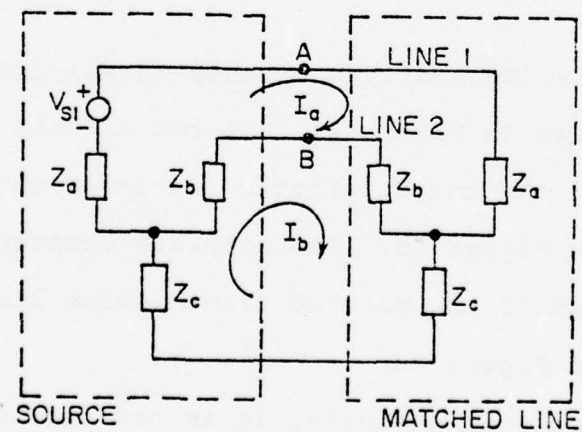
By circuit analysis, it is not difficult to show that the loop currents of Figure 4c are as follows:



(a)



(b)



(c)

Figure 4. (a) Voltage-driven matched three-conductor transmission line, (b) Circuit representation of characteristic impedance matrix \bar{Z}_0 , (c) Circuit representation of matched three-conductor transmission line.

$$I_a = \frac{1}{2} V_{s1} z_{o2} / (z_{o1} z_{o2} - z_{om}^2)$$

$$I_b = \frac{1}{2} V_{s1} (z_{o2} - z_{om}) / (z_{o1} z_{o2} - z_{om}^2)$$

The voltage of line 1 at $z = 0$, i.e., the voltage at point A is given by

$$V_1(0) = -I_b z_{om} + V_{s1} - I_a (z_{o1} - z_{om}) = \frac{1}{2} V_{s1}$$

Similarly, the voltage of line 2 at $z = 0$, i.e., at point B, is

$$V_2(0) = -I_b z_{om} - (I_b - I_a) (z_{o2} - z_{om}) = 0$$

The line currents are given by

$$I_1(0) = I_a = \frac{1}{2} V_{s1} z_{o2} / (z_{o1} z_{o2} - z_{om}^2)$$

$$I_2(0) = I_b - I_a = -\frac{1}{2} V_{s1} z_{om} / (z_{o1} z_{o2} - z_{om}^2)$$

These results are identical to those of (20).

(b) Short-Circuit Loads

An interesting coupling property is observed for the voltage-driven transmission line when all the source

and load impedances are just short-circuits to the reference conductor. Under these conditions, from (9), it can readily be shown that

$$\bar{I}_s = -\bar{U}_2$$

$$\bar{I}_l = -\bar{U}_2$$

and (8) becomes

$$\bar{V}(z) = \{[e^{-\gamma z} - e^{\gamma(z-2l)}]/(1 - e^{-2\gamma l})\} \bar{V}_s.$$

The last equation indicates that the line voltages are not cross-coupled to the driving voltage sources.

2. Numerical Results

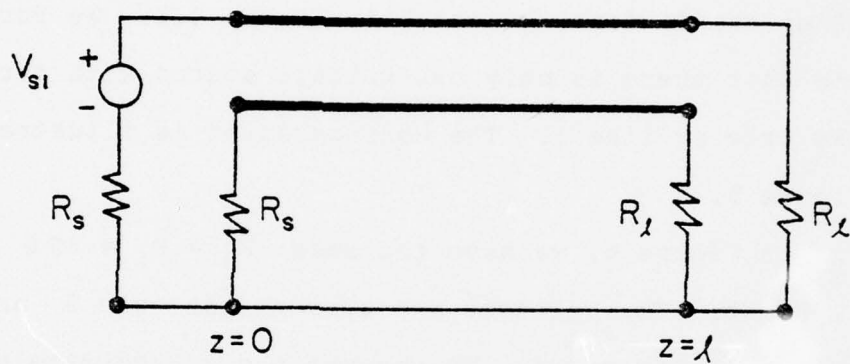
Numerical results are obtained for the voltage-driven transmission lines by evaluating (8). Two sets of results are presented here: One shows the terminal voltages and currents as a function of the coupling coefficient at a fixed frequency; the other shows the same quantities as a function of frequency for a fixed coupling coefficient.

For all the cases studied here, the transmission lines are 1 meter long. The elements of the characteristic

impedance matrix $\bar{\bar{Z}}_0$ are $Z_{01} = Z_{02} = 50 \Omega$. The source and load impedances contain simple resistances R_s and R_ℓ , respectively, connecting the conductors to the reference conductor, i.e., the off-diagonal elements of $\bar{\bar{Z}}_s$ and $\bar{\bar{Z}}_\ell$ are zero. In the first set of results, the frequency is chosen to be 100 MHz; in the second set, the coupling coefficient k is chosen to be 0.1. We further assume that there is only one voltage source with strength 1 volt driving line 1. The configuration is illustrated in Figure 5.

In Figure 6, we have the case $R_s = R_\ell = 50 \Omega$ at $f = 100$ MHz. The voltages and currents at $z = 0$ are presented in Figure 6a. We observe the approximately linear increase in the induced V, I on line 2 at low k . In Figure 6b, the voltages at $z = \ell$ ($= 1$ m) are presented. The vanishingly small induced voltage on line 2 at low k makes this configuration to be used as directional couplers (ref. 7). The currents at $z = \ell$ are simply related to the respective voltages by the resistances and are not presented.

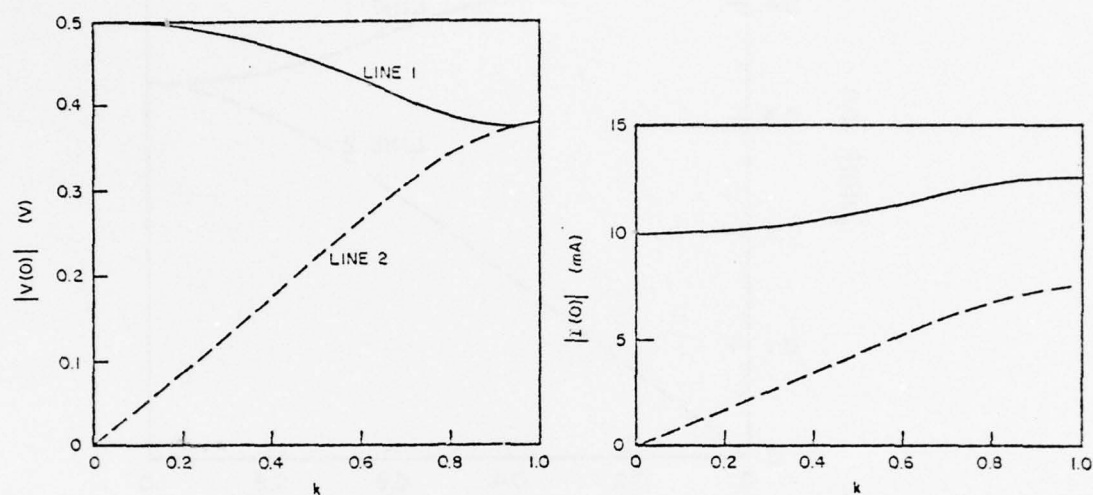
In Figure 7, we present the case that $R_s = 50 \Omega$ and $R_\ell = 100 \Omega$. The induced voltage on line 2 at $z = \ell$ is considerably higher than the previous case.



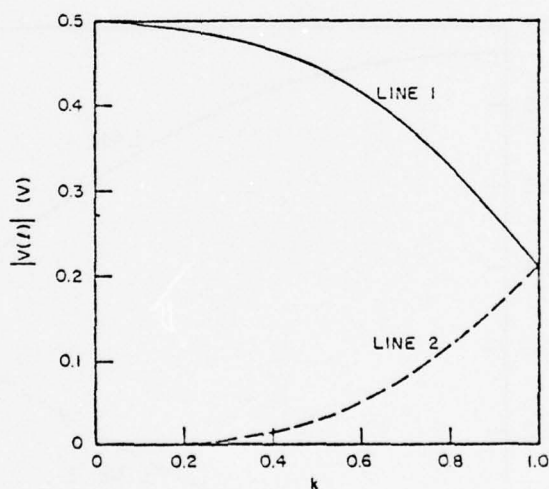
$$V_{s1} = 1V$$

$$\bar{\bar{Z}}_0 = \begin{bmatrix} 50 & Z_{om} \\ Z_{om} & 50 \end{bmatrix} \Omega$$

Figure 5. Three-conductor transmission line configurations for numerical studies.



(a)



(b)

Figure 6. The Case $R_S = R_L = 50\Omega$ at 100 MHz.
 (a) Voltages and Currents at $z=0$.
 (b) Voltages at $z=l$.

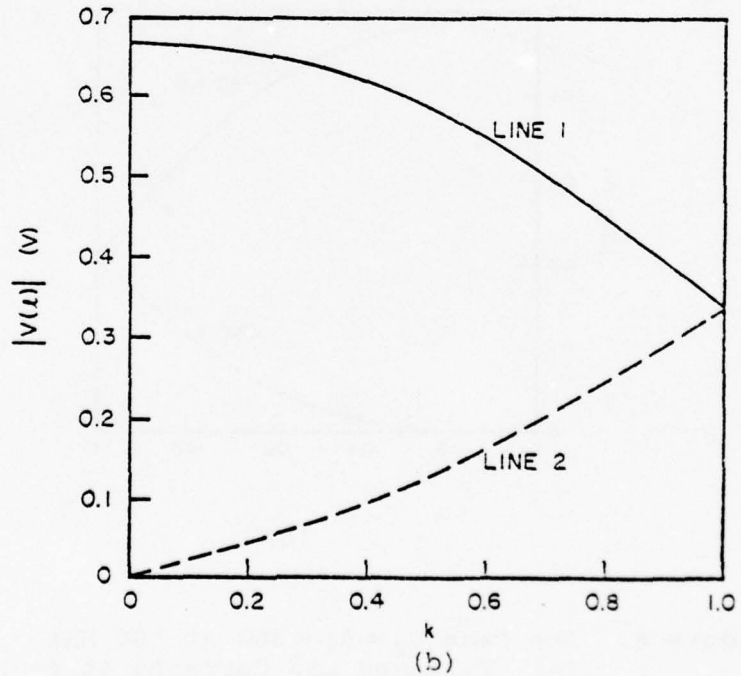
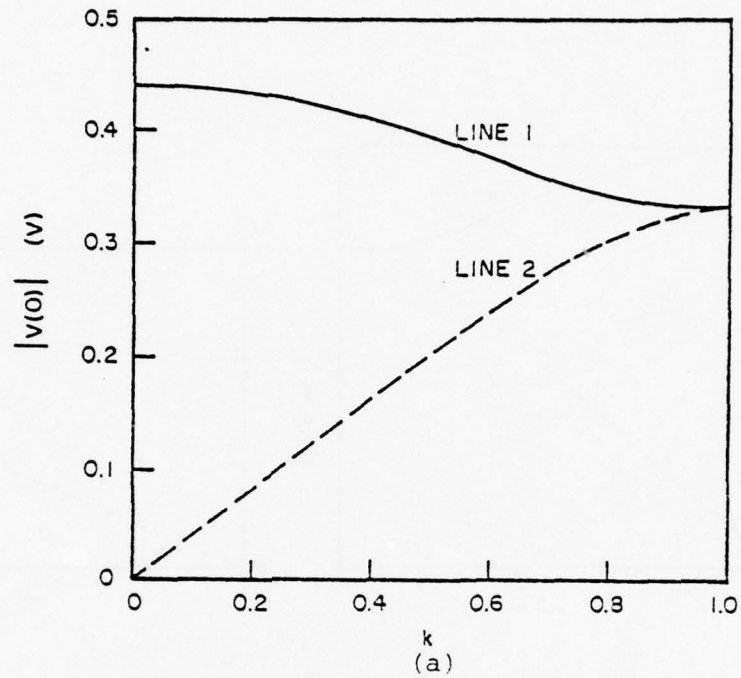
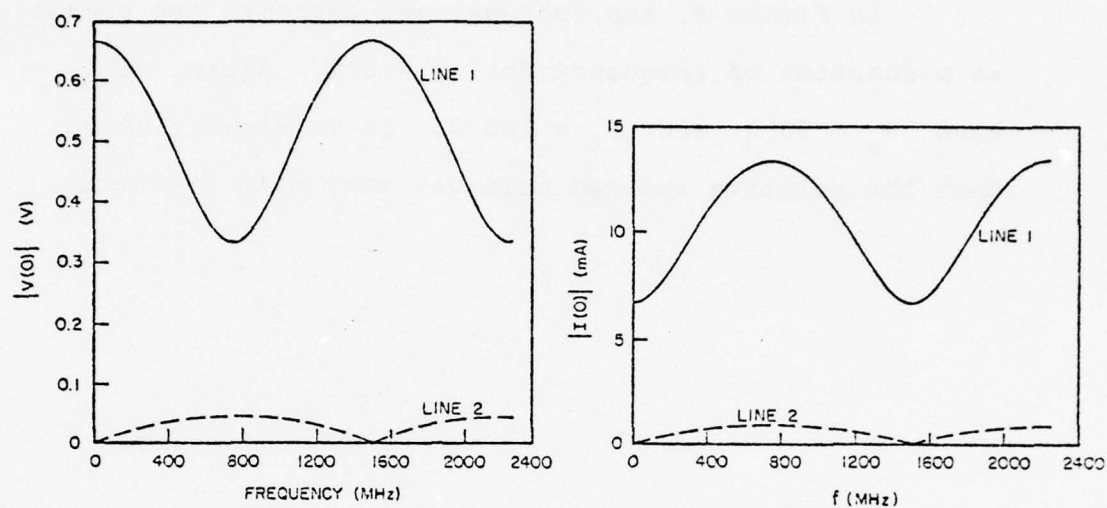
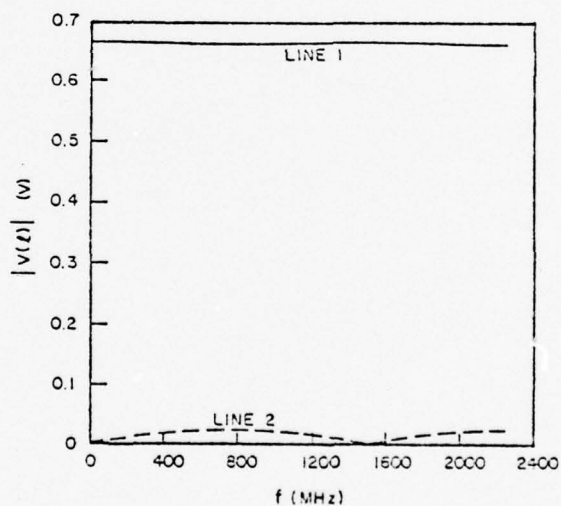


Figure 7. The case $R_s = 50\Omega$, $R_L = 100\Omega$ at 100 MHz.
 (a) Voltages at $z=0$.
 (b) Voltages at $z=l$.

In Figure 8, the voltages and currents are presented as a function of frequency for $k = 0.1$. Again, we have $R_s = 50 \, \Omega$ and $R_\ell = 100 \, \Omega$. It is clearly shown that the relative induced voltages vary with frequency.



(a)



(b)

Figure 8. The Case $R_s = 50\Omega$, $R_l = 100\Omega$ for $k=0.1$.
 (a) Voltages and Currents at $z=0$.
 (b) Voltages at $z=l$.

SECTION IV

EQUIVALENT GENERATORS REPRESENTATION OF CROSS-COUPLING

In this section we discuss the representation of the effect of voltages and currents of one line on another line by discrete equivalent voltage and current generators on the second line.

The rigorous approach is to solve the set of differential equations (1) and cast the solutions of the voltages and currents on one line in the same form as those of a single line containing discrete generators. However, the solutions of (1) are much too complicated for this purpose and simplifying assumptions must be made.

To simplify the problem, we assume that the induced line voltages and currents are small so that their effects on the exciting line are negligible. This assumption demands that the coupling between the two lines is weak. Later in this section, the accuracy of this assumption will be examined.

Under the assumption of weak coupling, it is sufficient to investigate only three-conductor transmission lines. For more than three conductors, the principle of superposition applies.

1. Formulation

For a loosely coupled three-conductor transmission line with both ends terminated in simple impedances, as in Figure 9, under the assumption made above, (1) can be re-written as

$$\frac{d V_1(z)}{dz} + s L_{11} I_1(z) \approx 0 \quad (21)$$

$$\frac{d I_1(z)}{dz} + s C_{11} V_1(z) \approx 0$$

$$\frac{d V_2(z)}{dz} + s L_{22} I_2(z) = - s L_m I_1(z) \quad (22a)$$

$$\frac{d I_2(z)}{dz} + s C_{22} V_2(z) = s C_m V_1(z) \quad (22b)$$

Equations (21) indicate that line 1 is not influenced by line 2, as assumed. However, (22) state that line 2 is influenced by two sources due to voltages and currents on line 1. When compared with the equations of a transmission line excited by external fields (ref. 3), the right-hand-side of (22a) can be represented by an electric field $E_e(z)$ and that of (22b) by a magnetic field $H_e(z)$, i.e.,

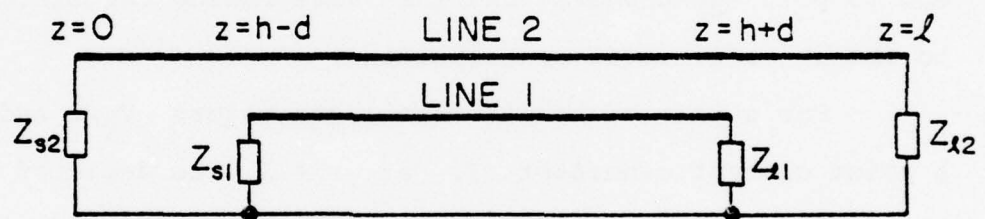


Figure 9. Three-conductor transmission line terminated in simple impedances.

$$\begin{aligned}
\frac{d V_2(z)}{dz} + s L_{22} I_2(z) &= E_e(z) = -s L_m I_1(z) \\
\frac{d I_2(z)}{dz} + s C_{22} V_2(z) &= H_e(z) = s C_m V_1(z)
\end{aligned}
\tag{23}$$

Equations (23) state that line 2 is excited by electric and magnetic fields maintained along the conductors. These fields are equivalent to a continuous distribution of voltage and current generators (ref. 8). Equations (23) can be solved by first obtaining the Green's function (i.e., due to point generators) and then integrating the fields to obtain their total contributions.

For a pair of point voltage generators $V_\xi/2$ and a point current generator I_ξ at $z = \xi$, as depicted in Figure 10, the line voltage and current are given by:

for $z \geq \xi$

$$\begin{aligned}
V(z) &= \frac{1}{2} \frac{e^{-\gamma z} + \rho_{\lambda 2} e^{\gamma(z-2\ell)}}{1 - \rho_{s2} \rho_{\lambda 2} e^{-2\gamma\ell}} \left[V_\xi (e^{\gamma\xi} - \rho_{s2} e^{-\gamma\xi}) \right. \\
&\quad \left. + Z_{o2} I_\xi (e^{\gamma\xi} + \rho_{s2} e^{-\gamma\xi}) \right] \\
I(z) &= \frac{1}{2 Z_{o2}} \frac{e^{-\gamma z} - \rho_{\lambda 2} e^{\gamma(z-2\ell)}}{1 - \rho_{s2} \rho_{\lambda 2} e^{-2\gamma\ell}} \left[V_\xi (e^{\gamma\xi} - \rho_{s2} e^{-\gamma\xi}) \right. \\
&\quad \left. + Z_{o2} I_\xi (e^{\gamma\xi} + \rho_{s2} e^{-\gamma\xi}) \right]
\end{aligned}
\tag{24}$$

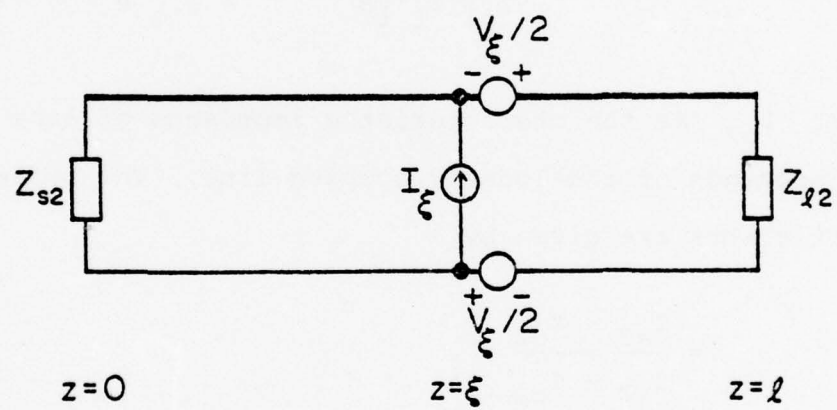


Figure 10. A pair of voltage generators $V_\xi/2$ and a current generator I_ξ at $z = \xi$.

for $z \leq \xi$

$$\begin{aligned}
 V(z) &= \frac{1}{2} \frac{e^{\gamma(z-l)} + \rho_{s2} e^{-\gamma(z+l)}}{1 - \rho_{s2} \rho_{l2} e^{-2\gamma l}} \left\{ -V_{\xi} \left[e^{\gamma(l-\xi)} - \rho_{l2} e^{-\gamma(l-\xi)} \right] \right. \\
 &\quad \left. + Z_{o2} I_{\xi} \left[e^{\gamma(l-\xi)} + \rho_{l2} e^{-\gamma(l-\xi)} \right] \right\} \\
 I(z) &= \frac{1}{2 Z_{o2}} \frac{e^{\gamma(z-l)} - \rho_{s2} e^{-\gamma(z+l)}}{1 - \rho_{s2} \rho_{l2} e^{-2\gamma l}} \left\{ -V_{\xi} \left[e^{\gamma(l-\xi)} - \rho_{l2} e^{-\gamma(l-\xi)} \right] \right. \\
 &\quad \left. + Z_{o2} I_{\xi} \left[e^{\gamma(l-\xi)} + \rho_{l2} e^{-\gamma(l-\xi)} \right] \right\} \quad (25)
 \end{aligned}$$

Here, Z_{o2} is the characteristic impedance of line 2 in the presence of the loosely coupled line. The reflection coefficients are given by

$$\begin{aligned}
 \rho_{s2} &= \frac{Z_{s2} - Z_{o2}}{Z_{s2} + Z_{o2}} \\
 \rho_{l2} &= \frac{Z_{l2} - Z_{o2}}{Z_{l2} + Z_{o2}}
 \end{aligned}$$

For line 1 coupled to line 2 from $z = h-d$ to $z = h+d$, as illustrated in Figure 9, we obtain

for $z \geq h+d$

$$\begin{aligned}
 V_2(z) &= \frac{1}{2} \frac{e^{-\gamma z} + \rho_{l2} e^{\gamma(z-2\ell)}}{1 - \rho_{s2} \rho_{l2} e^{-2\gamma\ell}} \int_{h-d}^{h+d} \left[E_e(\xi) (e^{\gamma\xi} - \rho_{s2} e^{-\gamma\xi}) \right. \\
 &\quad \left. + Z_{o2} H_e(\xi) (e^{\gamma\xi} + \rho_{s2} e^{-\gamma\xi}) \right] d\xi \\
 I_2(z) &= \frac{1}{2 Z_{o2}} \frac{e^{-\gamma z} - \rho_{l2} e^{\gamma(z-2\ell)}}{1 - \rho_{s2} \rho_{l2} e^{-2\gamma\ell}} \int_{h-d}^{h+d} \left[E_e(\xi) (e^{\gamma\xi} - \rho_{s2} e^{-\gamma\xi}) \right. \\
 &\quad \left. + Z_{o2} H_e(\xi) (e^{\gamma\xi} + \rho_{s2} e^{-\gamma\xi}) \right] d\xi \quad (26)
 \end{aligned}$$

Making use of definitions (23) for E_e and H_e , and also (16) so that $L_m I_1^+ / C_m Z_{o2} V_1^+ = 1$ for forward travelling waves on line 1, and $L_m I_1^- / C_m Z_{o2} V_1^- = -1$ for backward travelling waves, then (26) become

$$\begin{aligned}
 V_2(z) &= \frac{e^{-\gamma z} + \rho_{l2} e^{\gamma(z-2\ell)}}{1 - \rho_{s2} \rho_{l2} e^{-2\gamma\ell}} \frac{C_m}{C_{22}} \sinh(2\gamma d) \\
 &\quad \times \left[\rho_{s2} V_1^+ e^{-2\gamma h} + V_1^- e^{2\gamma h} \right] \\
 I_2(z) &= \frac{1}{Z_{o2}} \frac{e^{-\gamma z} - \rho_{l2} e^{\gamma(z-2\ell)}}{1 - \rho_{s2} \rho_{l2} e^{-2\gamma\ell}} \frac{C_m}{C_{22}} \sinh(2\gamma d) \\
 &\quad \times \left[\rho_{s2} V_1^+ e^{-2\gamma h} + V_1^- e^{2\gamma h} \right] \quad z \geq h+d \quad (27)
 \end{aligned}$$

Similar expressions are derived for $z \leq h-d$:

$$V_2(z) = \frac{e^{\gamma(z-l)} + \rho_{s2} e^{-\gamma(z+l)}}{1 - \rho_{s2} \rho_{l2} e^{-2\gamma l}} - \frac{C_m}{C_{22}} \sinh(2\gamma d)$$

$$\left[V_1^+ e^{\gamma(l-2h)} + \rho_{l2} V_1^- e^{-\gamma(l-2h)} \right]$$

$$I_2(z) = \frac{1}{z_{o2}} \frac{e^{\gamma(z-l)} - \rho_{s2} e^{-\gamma(z+l)}}{1 - \rho_{s2} \rho_{l2} e^{-2\gamma l}} - \frac{C_m}{C_{22}} \sinh(2\gamma d)$$

$$\left[V_1^+ e^{\gamma(l-2h)} + \rho_{l2} V_1^- e^{-\gamma(l-2h)} \right]$$

$$z \leq h-d \quad (28)$$

Equations (27) and (28) can also be obtained by placing appropriate discrete generators on line 2 to represent the effect of coupling. A few possible representations are shown in Figure 11. In Figure 11a, two pairs of generators of opposite signs are placed at $z = h-d$ and $z = h+d$ with total magnitude

$$V_a = (C_m/C_{22}) \cosh(\gamma d) (V_1^+ e^{-\gamma h} + V_1^- e^{\gamma h}) \quad (29)$$

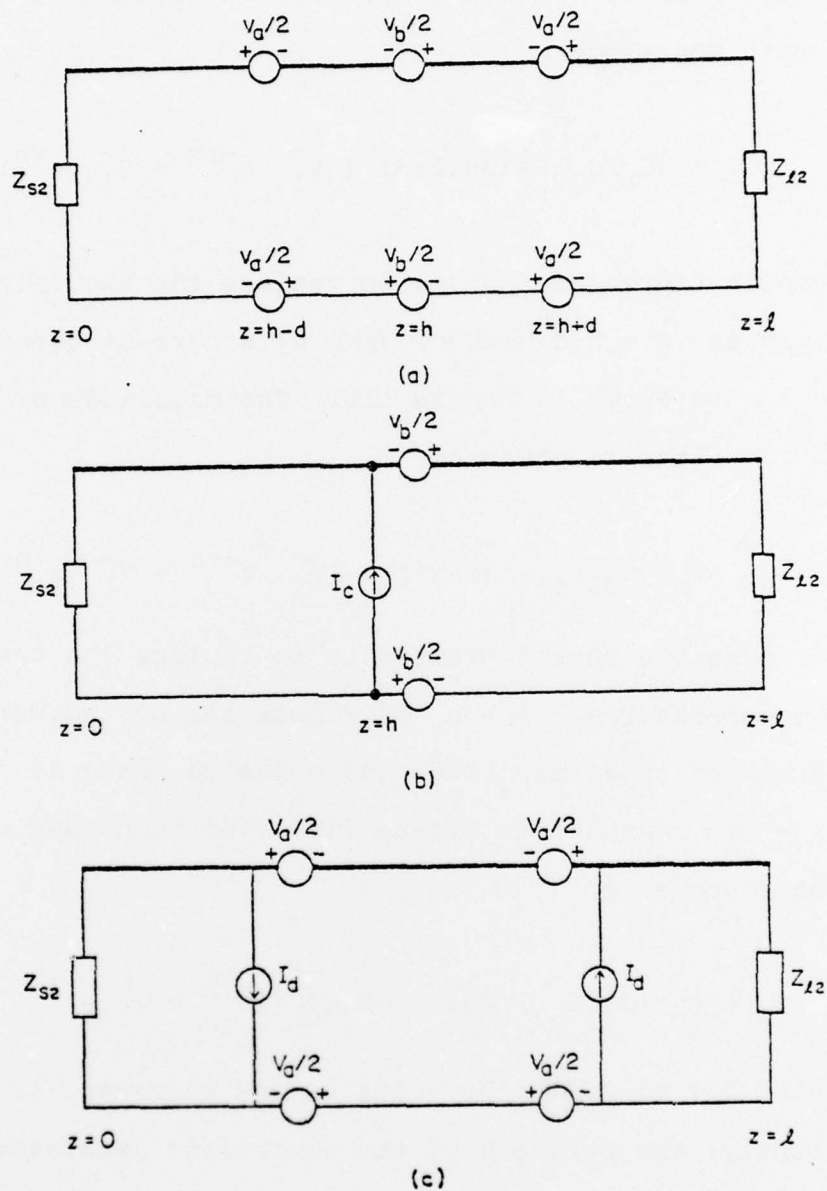


Figure 11. Three possible equivalent generator representations of cross-coupling:
 (a) three voltage generators,
 (b) one voltage and one current generators, and
 (c) two voltage and two current generators.

and another pair of voltage generators is located at $z = h$ with magnitude

$$V_b = (C_m/C_{22}) \sinh(2\gamma d) (-V_1^+ e^{-\gamma h} + V_1^- e^{\gamma h}) \quad (30)$$

An alternate representation is to replace the two pairs of generators at $z = h-d$ and $z = h+d$ by a current generator at $z = h$, as shown in Figure 11b. The magnitude of the current generator is given by

$$I_c = C_m/(C_{22}Z_{02}) \sinh(2\gamma d) (V_1^+ e^{-\gamma h} + V_1^- e^{\gamma h}) \quad (31)$$

Another possible representation is to replace the center voltage generator at $z = h$ of Figure 11a by two current generators of equal magnitude and opposite phase at $z = h-d$ and $z = h+d$, as shown in Figure 11c. The magnitude of the current sources is

$$I_d = C_m/(C_{22}Z_{02}) \cosh(\gamma d) (-V_1^+ e^{-\gamma h} + V_1^- e^{\gamma h}) \quad (32)$$

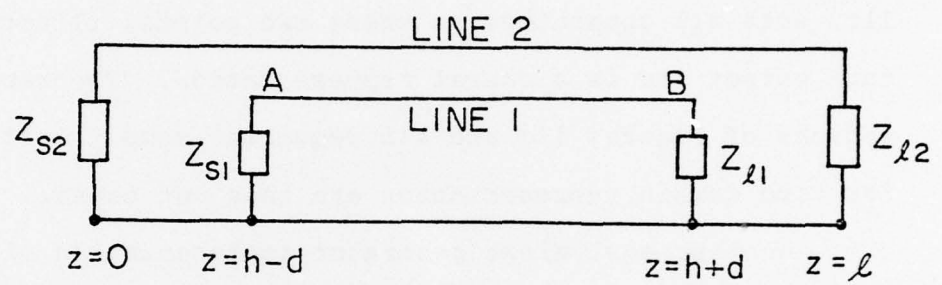
In (27) to (32), the voltages and currents, or equivalently, the strength of the equivalent generators on line 2, depend on the magnitude of the forward and backward travelling waves on line 1, V_1^+ and V_1^- . These two quantities are easily calculated for the unperturbed line 1 for a given excitation.

A comment on the causality of the equivalent generator representations should be made here. As line 1 directly excites line 2 at $z = h-d$ and $z = h+d$, for a transient excitation, energy should start propagating on line 2 from these two points. Thus, the representation of Figure 11c, with all generators at these two points, illustrates this effect and is a causal representation. The representations of Figures 11a and 11b requiring some time delay for time domain representation are thus not causal.

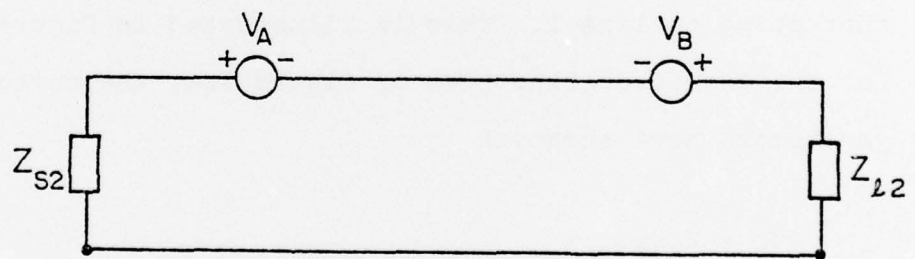
Another equivalent generator representation of the effect of line 1 on line 2 has been suggested by Boeing recently (ref. 9). Equivalent voltage generators are placed on line 2 at positions where line 1 has discontinuities with strength being proportional to the line voltage at that point on line 1. This is illustrated in Figure 12. For the two discontinuities of Figure 12a, the voltage generators have strength

$$\begin{aligned} V_A &= K V_1(\xi_A) \\ V_B &= K V_1(\xi_B) \end{aligned} \tag{33}$$

and have opposite polarities. Here, K is an empirical constant measured in experiments, $V_1(\xi_A)$ is the line voltage on line 1 at position A.



(a)



(b)

Figure 12. Two voltage generator representation of effect of voltage and current of line 1 on line 2.

The line voltages and currents for line 2 due to the two voltage generators (see Figure 12b) can be readily evaluated; the voltage is given by

$$V_2(z) = \frac{1}{2} \frac{e^{-\gamma z} + \rho_{\ell 2} e^{\gamma(z-2\ell)}}{1 - \rho_{s2} \rho_{\ell 2} e^{-2\gamma\ell}} \left[e^{\gamma h} (-V_A e^{-\gamma d} + V_B e^{\gamma d}) - \rho_{s2} e^{-\gamma h} (-V_A e^{\gamma d} + V_B e^{\gamma d}) \right]$$

$$z \geq h+d \quad (34)$$

Decomposing V_1 into forward and backward travelling waves with magnitude V_1^+ and V_1^- , respectively, substitution of (33) into (34) yields,

$$V_2(z) = \frac{e^{-\gamma z} + \rho_{\ell 2} e^{\gamma(z-2\ell)}}{1 - \rho_{s2} \rho_{\ell 2} e^{-2\gamma\ell}} K \sinh(2\gamma d) \left[\rho_{s2} V_1^+ e^{-2\gamma h} + V_1^- e^{2\gamma h} \right]$$

$$z \geq h+d \quad (35)$$

Comparison with (27) shows that

$$K = C_m / C_{22} \quad .$$

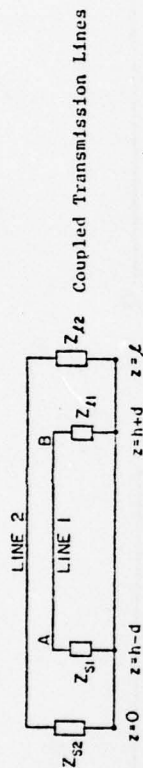
The two-voltage generator representation with V_A and V_B at $z = h-d$ and $z = h+d$, respectively, is a causal representation.

In Table I, all the four representations (Figures 11 and 12) are summarized.

2. Comparison with Exact Theory

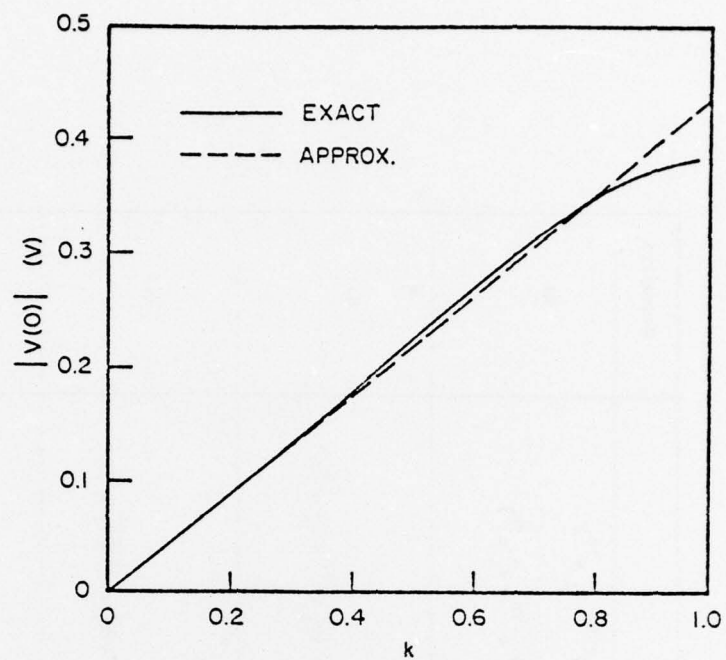
By comparing the results obtained by evaluating the appropriate solution (27) with that by evaluating (8), it is possible to see how good the assumptions are in deriving (27). Ideally one expands (8) in terms of a series in the coupling coefficient k and observes the errors when higher order k terms are dropped. However, such an analytical task is far too involved even for a three-conductor transmission line. Numerical comparisons are used.

We use the same line parameters as those used in Section III.2. Here we compare the induced voltages on line 2 as a function of the coupling coefficient k at 100 MHz. In Figure 13a, the case $R_S = R_\lambda = 50 \Omega$ is presented and in Figure 13b, the case $R_S = 50 \Omega$ and $R_\lambda = 100 \Omega$. We observe that the approximate theory is good up to $k \approx 0.5$.

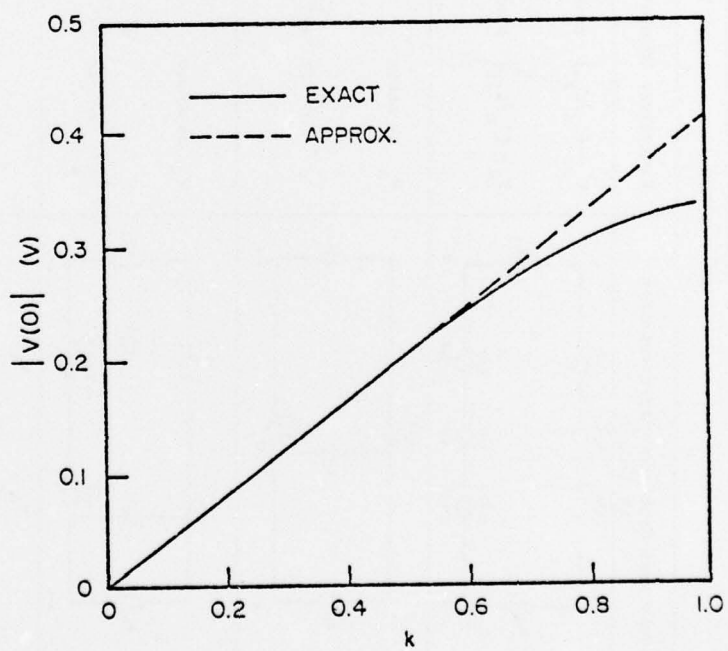


Equivalent Generator Representation on line 2	Equivalent Generators	Causality
	$V_a = (C_m / C_{22}) \cosh(\gamma d) (V_1^+ e^{-\gamma h} + V_1^- e^{\gamma h})$ $V_b = (C_m / C_{22}) \sinh(2\gamma d) (-V_1^+ e^{-\gamma h} + V_1^- e^{\gamma h})$	No
	V_b as above $I_c = C_m / (C_{22} Z_{o2}) \sinh(2\gamma d) (V_1^+ e^{-\gamma h} + V_1^- e^{\gamma h})$	No
	V_a as above $I_d = C_m / (C_{22} Z_{o2}) \cosh(\gamma d) (-V_1^+ e^{-\gamma h} + V_1^- e^{\gamma h})$	Yes
	$V_A = (C_m / C_{22}) V_1(\epsilon_A)$ $V_B = (C_m / C_{22}) V_1(\epsilon_B)$	Yes

Table I. Summary of equivalent generator representations.



(a)



(b)

Figure 13. Comparisons of exact and approximate results.
(a) $R_S = R_L = 50\Omega$, and (b) $R_S = 50\Omega$ and $R_L = 100\Omega$.

SECTION V

CONCLUSIONS

The coupling between conductors for a multi-conductor transmission line immersed in a homogeneous medium have been studied. The special case of a three-conductor transmission line has been investigated in detail. It has been shown that for small coupling the effect of energy of one line on another can be represented by some discrete equivalent generators on the induced line: three voltage generators; one voltage generator and one current generator; two voltage generators and two current generators, or two voltage generators.

For a multiconductor transmission line in an inhomogeneous medium, the responses will be different to those described in this report. It is expected that the small coupling theory will not be adequate if the differences in the mode velocities are large. This may indeed be a worthwhile problem to investigate.

REFERENCES

1. C.R. Paul, "On uniform multimode transmission lines," IEEE Trans. Microwave Theory Tech., Vol. MTT-21, pp. 556-558, August 1973.
2. S. Ramo, J.R. Whinnery, and T. Van Duzer, Fields and Waves in Communication Electronics, Wiley, New York, 1965.
3. S. Frankel, "Cable and multiconductor transmission line analysis," Harry Diamond Laboratory, Tech. Rept. HDL-TR-091-1, June 1974.
4. D. Kajfez, "Multiconductor transmission lines," AFWL Interaction Note 151, June 1972.
5. ITT, Reference Data for Radio Engineers, 6th Ed., H.W. Sams & Co., 1975.
6. C.A. Desoer and E.S. Kuh, Basic Circuit Theory, McGraw-Hill, 1969.
7. B.M. Oliver, "Directional electromagnetic couplers," Proc. IRE, Vol. 42, pp. 1686-1692, Nov. 1954.
8. R.W.P. King, Transmission-Line Theory, Dover, 1965.
9. J.M. Carter, E.J. Pultorak, G.L. Maxam, and M.L. Vincent, "Electromagnetic pulse internal coupling technology," Boeing Report D224-13061-1, April 1975.

DISTRIBUTION

Arnold Research Orgn, Inc., Lib-Tech Document/ W.G. Kirby Arnold AFS TN 37389	USAF/RDPE/Maj A. Bills Wash D C 20331	1
Aeronautical Sys Division ENFTV/Capt Guice Wright-Patterson AFB OH 45433	The Boeing Co. ATTN: W. Levens, Seattle WA 98124	1
AFAPL/POD/D. Fox Wright-Patterson AFB OH 45433	1 US Dept of Commerce/ITS/OT ATTN: Dr D. Hill/Rm 1-2237 Dr J. Wait/Rm 3017	2
RADC/EPER/R. Mack L. G. Hanscom AFB MA 01731	1 Boulder CO 80302	1
AFFDL/FGL/G. DuBro Wright-Patterson AFB OH 45433	DASIAC/GE TEMPO/Dr Reitz 1 Santa Barbara CA 93102	1
AFIT/ENE/Lt W. Davis, Elec Engr Dept Wright-Patterson AFB OH 45433	Def Adv Research Proj Agcy 1 ATTN: Dr E. Blase, Arlington VA 22209	1
AFGL/OPR/Lt J. Little L. G. Hanscom AFB MA 01730	DNA/RAEV/Capt D. Wilson, Wash DC	1
AFML/LG/R. Neff Wright-Patterson AFB OH 45433	1 Dikewood Ind Inc., ATTN: Jiunn Yu/B. Singaraju	2
AFOSR/NP/Lt Col G. Wepfer Physics Prog/Bldg 410 Bolling AFB D C 20332	1 Albuquerque NM 87106	2
AF/FTD/ETET/Mr B. Ballard Wright-Patterson AFB OH 45433	Dikewood Ind, Inc., Westwood Br 1 ATTN: Dr K. Lee/Dr L. Marin	2
AMSEL-TL-ENV/Dr. H. Bomke US Army Elec Cmd, Ft Monmouth NJ 07703	Los Angeles CA 90024	1
AMSEL-KL-TG/W. Wright, Jr. Ft Monmouth NJ 07703	ESD/YWED/Maj Royer/YSEV/Capt West 2 L. G. Hanscom AFB MA 01730	2
US Army Missiles Cmd AMSMI-RGP/H. Greene Redstone AL 35809	Sidney Frankel & Assoc 1 Menlo Park CA 94025	1
US Army Safeguard Sys Office ATTN: C. Old, Arlington VA 22209	GTE Sylvania Comm Sys Div 1 ATTN: Mr Perlman, Needham MA 02194	1
Cmdg Gen, US Army Strategic Comm Cmd ACC-OPS-PD/C. Brewington Ft Huachuca AZ 85613	Cmdg Off, Harry Diamond Labs 1 AMXDC-EM/Dr J. Bombardt	1
ASD/YH/EV/Capt C. Hale Wright-Patterson AFB OH 45433	Adelphi MD 20783	1
	U of Ill, Dept of EE/Prof R Mittra	1
	1 Urbana IL 61801	1
	Kaman Sciences Corp/Dr W. Ware	1
	1 Colorado Springs CO 80907	1
	Kansas State University	2
	ATTN: EE Dept/Prof K. Casey	2
	1 Math Dept/ Dr C. Yee	2
	Manhattan, KS 66506	2
	1 LRL, Livermore Div/Dr A. Poggio	1
	Livermore CA 94551	1

Lawrence Berkeley Lab, U of Calif, ATTN: Dr A. Sessler Berkeley, CA 94720	1	Ogden/ALC/MMETH/Maj R. Blackburn Hill AFB UT 84406	1
Lightning Transient Research Institute ATTN: J. Robb, St Paul MN 55113	1	R&D Assoc/Tech Library Marina del Ray CA 90291	1
LASL, J-DOT/Dr J. Malik Los Alamos, NM 87544	1	RADC/RBCT/K. Siarkiewicz Griffis AFB NY 13441	1
MIT Lincoln Lab/Tech Lib, L. Loughlin Lexington, MA 02191	1	Sandia Labs/R. Parker Albuquerque NM 87115	1
U of Mich, Radiation Lab Dept ECE/Prof C. Tai Ann Arbor, MI 48104	1	Science Applications, Inc. ATTN: Dr F. Tesche Berkeley CA 94701	5
Michigan State University Dept of EE/M. Siegel E. Lansing MI 48823	1	SAMSO/MNNH-MNS-1, Maj M. Baran Norton AFB CA 92409	1
Mission Research Corp ATTN: D. Merewether Dr A. Chodorow Library Albuquerque NM 87108	3	1 Stanford Research Institute ATTN: E. Vance Ft Worth, TX 76119	1
Mission Research Corp ATTN: Dr C. Longmire Santa Barbara, CA 93102	1	TDR, Inc., M. Sancer Los Angeles CA 90049	1
Mississippi State University ATTN: C. Taylor, Physics Dept State College, MS 39762	1	USAF, AFTAC/TAP Patrick AFB FL 32925	1
U of Mississippi/Dept of EE, Dr Butler, University MS 38677	1	USAF/RDQSM, 1D425, Wash D C 20330	1
Naval Surface Wpns Cen Code DF-12/Dr R. Wasneski Dahlgren VA 22448	1	AFSC/DLCAW, Andrews AFB MD 20334	1
Naval Elec Lab Cen/Code 2110 Dr J. Rockway, San Diego CA 92152	1	1 AUL/LDE, Maxwell AFB AL 36112	1
Naval Postgraduate School NC4(023A)/Lt Col R. Burton Monterey CA 93940	1	AFIT/Tech Lib, Wright-Patterson 1 AFB OH 45433	1
Naval Surface Wpns Cen Phys Dept/L. Libelo White Oak, MD 20910	1	USAF, SCLO (Ch LO/Maj Pierson) POB 348, Toronto ON Canada M5K 1K7	1
Naval Research Lab/J. Shipman Wash D C 20375	1	USAF/DFSLB and FJSRL/CO 80840	2
	1	AFFDL(DOO/Lib) Wright-Patterson AFB OH 45433	1
	1	AFGL, L. G. Hanscom AFB MA 01730	1
	1	RADC/Doc Lib/Griffiss AFB, NY 13441	1
	1	AFRPL/DYSN/Edwards AFB, CA 93523	1
	1	LLL/Lib/Berkeley CA 94720	1
	1	1 Dir/LASL, Los Alamos NM 87545	1

AFWL-TR-76-333

DDC/TCA/Cameron Sta Alexandria, VA 22314	2
---	---

Science Applications Inc. Berkeley CA 94701	1
--	---

AFWL, Kirtland AFB NM 87117

SUL	2
HO/Dr Minge	1
NT/Dr Payton	1
Dr Baum	2
Mr Darrah	1
EL/Tech File	1
ELA/Dr Castillo	1
Dr Chen	1
ELP/Capt Harrison	1
Capt Hudson	1
Mr Prather	1
Dr Page	1
Dr Giri	1
ELS/Capt Bonn	1
TPO/Mr Shover	1

Official Record Copy (AFWL/ELP/Capt Harrison, Kirtland AFB, NM 87117)	1
---	---